© 1973 IEEE. Personal use of this material is permitted. However, permission to reprint/republish this material for advertising or promotional purposes or for creating new collective works for resale or redistribution to servers or lists, or to reuse any copyrighted component of this work in other works must be obtained from the IEEE.

A METHOD OF ANALYZING THE MOMENTUM AND BETATRON* AMPLITUDE DISTRIBUTIONS IN A CIRCULATING BEAM

J.M. Peterson and J.B. Rechen

Lawrence Berkeley Laboratory
University of California
Berkeley, California

Summary

We have developed a two-probe method of analyzing the momentum and radial-betatron-amplitude distributions in a circulating particle beam. It has been used successfully in an electron-ring research program to help diagnose beam instabilities and injection techniques.

I. Introduction

The spatial distribution of particles in a circulating beam can be an important parameter to determine, for it is a major factor in the luminosity of an intersecting storage ring, for example, or in the holding power of an electron-ring accelerator. Also, a knowledge of the radial or axial width of a beam can often be used to diagnose a beam instability or the operation of the injection system.

The axial-density profile in a circulating beam is determined by its distribution in axial betatron amplitude ($A_{\beta z}$). The radial density profile, on the other hand, depends on both the distribution in radial betatron amplitude ($A_{\beta r}$) and the distribution in momentum (p) or, equivalently, closed-orbit radius (R_{co}).

Many methods and techniques can be employed for measuring the distribution of particles across a circulating beam. For example, the time dependence of the beam signal from a probe onto which the beam is slowly being swept axially gives the distribution of the beam in axial betatron amplitude ($A_{\beta z}$). If the sweep direction is radially outward, the signal gives the distribution in the combined parameter ($R_{co} + A_{\beta r}$). The spatial distribution of slow ions produced by the beam through ionization of the residual gas in the vacuum chamber can give an excellent one-dimensional beam density profile.[1] Very similarly the imaging of synchrotron light emitted by a circulating relativistic electron beam can produce a two-dimensional profile.[2] In addition, radio-frequency techniques can be used to determine momentum widths and betatron frequencies.

All of these methods of examining internal, circulating beams can be useful in determining the beam density. However, none by itself measures both the spread in momentum and the spread in betatron amplitude. We have developed an extension of the intercepting-probe method for measuring simultaneously the distributions in momentum and in betatron amplitude and their correlations. This technique is useful in electron ring work, where the momentum width and the betatron width typically are comparable in magnitude, and where it is often advantageous for diagnostic reasons to distinguish between them.

II. Two-Probe Method of Analysis

We shall describe a two-probe method for analyzing separately the distributions in particle momentum and in amplitude of radial betatron oscillation. One probe clips the beam at the inner radius, and the other at the outer radius. It is convenient to describe the procedure in terms of a closed-orbit-radius versus betatron-amplitude phase space, in which the dynamics of a particle in the beam can be represented by a point designating both its closed-orbit radius (and, hence, its momentum) and its amplitude of betatron oscillation. The dynamics in the radial plane of a circulating particle beam can thus be represented completely by the particle density function $\rho(R_{co},A_{\beta r})$ which includes the correlations between momentum and radial-betatron amplitude. The distributions in closed-orbit radius and in betatron amplitude $N_p(R_{co})$ and $N_\beta(A_{\beta r})$ are the projections of the density function on the two coordinate axes, as indicated in Figure 1.

The density function $\rho(R_{co},A_{\beta r})$ can be determined by the combined action of an inner probe at radius R_1, which intercepts those particles for which $(R_{co} - A_\beta) \leq R_1$, followed by an outer probe that is slowly brought in to a radius R_2, at which point it has intercepted all the remaining particles for which $(R_{co} + A_\beta) \geq R_2$. To illustrate the action of the probes it is convenient to transform from the $R_{co},A_{\beta r}$ coordinate system to the equivalent R_1,R_2 coordinate system. These systems are related by the transformation

$$R_{co} = (R_1 + R_2)/2$$

$$A_{\beta r} = (R_2 - R_1)/2$$

Since the Jacobian of this transformation $J(R_{co}, A_{\beta r}/R_1, R_2)$ is equal simply to 1/2, the density functions in the two systems are simply proportional to each other at corresponding points, as:

$$\sigma(R_1,R_2) = 1/2\ \rho(R_{co},A_{\beta r}).$$

This transformation, which is a 45° rotation and a stretching of the coordinate systems, is illustrated in Figure 2.

After the inner probe at R_1 has intercepted all particles having $(R_{co} - A_{\beta r}) \leq R_1$, those intercepted by the outer probe when it reaches R_2 is given by

$$N_2(R_1,R_2) = \int_{R_1}^{\infty} dR_1' \int_{R_2}^{\infty} \sigma(R_1',R_2')dR_2'$$

(Inclusion in this integral of the unphysical area where $R_1 > R_2$ is merely a notational convenience and contributes nothing to the integral.) Thus the density functions are given by the second derivative of $N_2(R_1,R_2)$ with respect to R_1 and R_2:

$$\sigma(R_1,R_2) = 1/2\ \rho(R_{co},A_{\beta r}) = \frac{\partial^2 N_2(R_1,R_2)}{\partial R_1\ \partial R_2}$$

To find the average particle density in real space one must in effect smear each particle over its range from $(R_{co} - A_{\beta r})$ to $(R_{co} + A_{\beta r})$. Thus the average number $n(R)$ of particles per unit radius at radius R is found by folding the phase-space-density function $\rho(R_{co},A_{\beta r})$ with the smearing function, as follows:

* Work supported by the U.S. Atomic Energy Commission.

$$n(R) = \frac{1}{2\pi}\int_0^\infty dR_{co} \int_{|R-R_o|}^\infty \frac{\rho(R_{co},A_{\beta r})dA_{\beta r}}{\left[A_{\beta r}^2 - (R_{co}-R)^2\right]^{1/2}}$$

III. Use of the Two-Probe Method

This two-probe method has been successfully used at the Lawrence Berkeley Laboratory to analyze the momentum and radial betatron distributions in electron rings in an electron-ring compressor system. In this system it is not practical to move mechanical probes appreciably during times of interest, so equivalently the beam is first moved slowly inward to be clipped on an inner probe at R_1 and then swept rather quickly (but adiabatically) outward until all the remaining beam particles are intercepted by the outer probe.

The time-dependent x-ray signal from the probe $X_2(R_1,t)$ is proportional to the gradient function $\partial N_2(R_1,R_2)/\partial R_2$ and the outward rate of motion of the beam dR_2/dt:

$$X_2(R_1,t) \propto \frac{\partial N_2(R_1,R_2)}{\partial R_2} \cdot \frac{dR_2}{dt}$$

The net outward velocity dR_2/dt produced by our radial sweeper system was measured to be approximately 2.8 cm/μsec and almost constant over the time interval of interest. The density function $\sigma(R_1,R_2)$ was found by taking consecutive differences between a series of $X_2(R_1,t)$ curves with ΔR_1 intervals of 0.25 cm. Such a series of $X_2(R_1,t)$ curves is illustrated in Figure 3. The resultant $\sigma(R_1,R_2)$ or $\rho(R_{co},A_{\beta r})$ data and the corresponding closed-orbit and radial-betatron-amplitude distributions are shown in Figure 4.

The inner probe used in this work had an unusual set of simultaneous requirements. Because we wished to analyze the electron ring before it compressed very far; the range of the inner probe radius R_1 had to extend into the injection region. In order not to interfere with the injection process nor with the growth of any prompt instability either through interception of the beam or through electrical images on the probe, the probe was made of a thin (0.05 cm x 0.05 cm) strip of high temperature plastic (vespel) that extended axially across the chamber, with a "catcher" plate some 4 cm farther inward, where the intercepted beam eventually dumped. This size probe could intercept only about 1% of the beam per turn, so that it did not seriously perturb the beam during the growth of the prompt instabilities, which developed usually within 10 turns or less. On the other hand, the probe was large enough to wipe out virtually all beam within its radius in less than 2 microseconds (560 turns). The radial sweeper was switched on normally at 10 microseconds after injection; it provided a sinusoidal magnetic bump with a 3 microsecond quarter period.

Two types of x-ray detectors have been used. A silicon-diode (type 25PIN2501E) detector built by C.D. Pike has been favored because of its nanosecond-type response time. At very low beam levels a more sensitive Pilot-B plastic scintillator-photomultiplier assembly built by D.R. George was successfully used, although its response time was somewhat longer. The radial sweeper was kindly provided by A. Faltens and J.A. Hinkson. We are indebted to J.R. Meneghetti and G.M. Webster for the delicate inner probe.

References

1. W.H. DeLuca, Beam Detection Using Residual Gas Ionization, Proc. of 1969 Particle Accelerator Conference, IEEE Trans. on Nuclear Science, NS-16, No. 3, 813 (June 1969).

2. D. Keefe, G.R. Lambertson, L.J. Laslett, W.A. Perkins, J.M. Peterson, A.M. Sessler, R.W. Allison, W.W. Chupp, A.U. Luccio, and J.B. Rechen, Experiments on Forming Intense Rings of Electrons Suitable for the Acceleration of Ions, Phys. Rev. Letters, 22, 558 (1969).

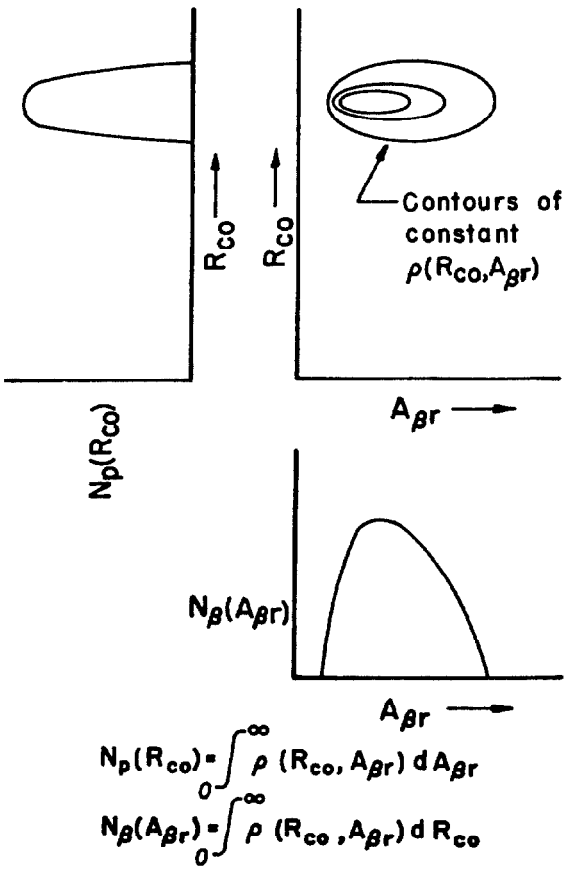


Fig. 1. A particle-density plot in R_{co},$A_{\beta r}$ phase space and the corresponding density distributions in closed-orbit radius and in radial-betatron amplitude.

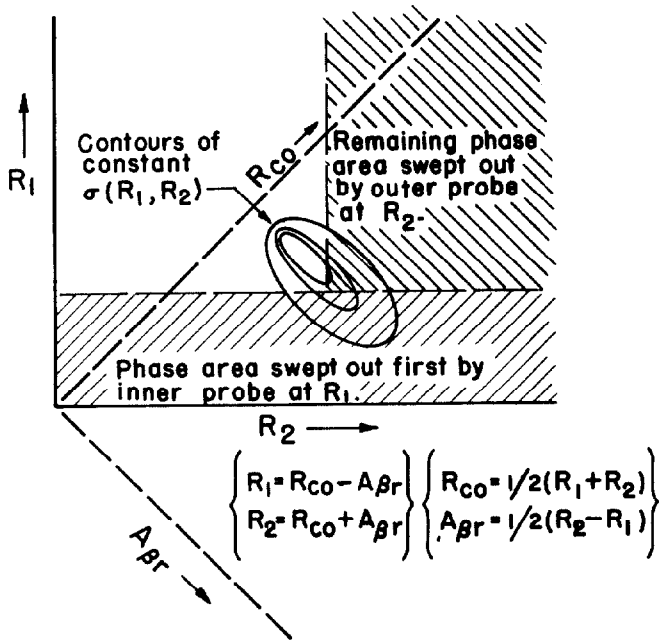


Fig. 2. The particle-density distribution of Figure 1 as transformed to the R_1,R_2 coordinate system. Note that all particles must be in the 45° sector common to the first quadrants of the two coordinate systems.

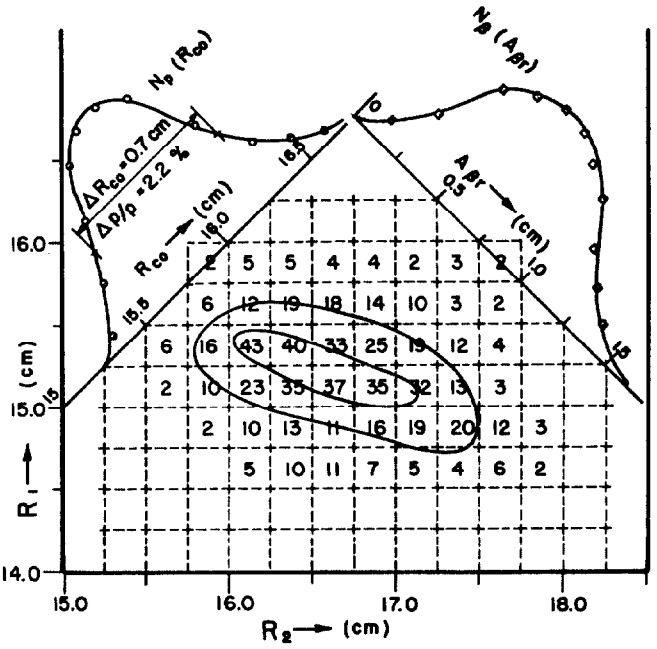


Fig. 4. The particle-density data $\sigma(R_1,R_2)$ derived from the $X_2(R_1,t)$ data of Figure 3, and the projections on the R_{co} and $A_{\beta r}$ axes to give the density distributions $N_p(R_{co})$ and $N_\beta(A_{\beta r})$.

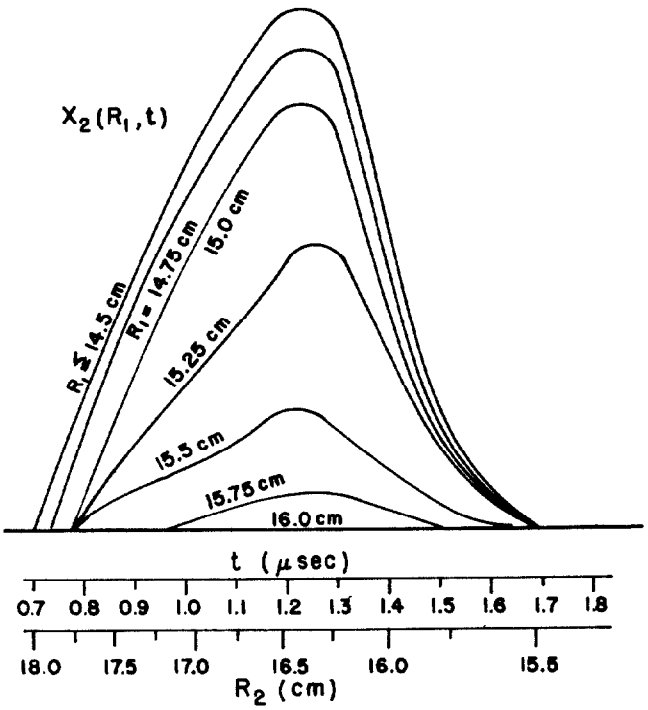


Fig. 3. An experimental X-ray signal $X_2(R_1,t)$. The R_2 coordinate corresponding to time t also is indicated.